1964

The transient response of the cesium diode to potential pulses

Hui-Ying Chung
Iowa State University

THE TRANSIENT RESPONSE OF THE CESIUM DIODE TO POTENTIAL PULSES

by

Hui-Ying Chung

A Dissertation Submitted to the

Graduate Faculty in Partial Fulfillment of

The Requirements for the Degree of

DOCTOR OF PHILOSOPHY

Major Subject: Electrical Engineering

Approved:

Signature was redacted for privacy.

In Charge of Major Work

Signature was redacted for privacy.

Head of Major Department

Signature was redacted for privacy.

Dean of Graduate College

Iowa State University
Of Science and Technology
Ames, Iowa

1964

TABLE OF CONTENTS

I. INTRODUCTION

Among the present day thermionic energy converters it appears that the cesium plasma cell is one of the most promising kind. However, by far its performance is considerably lower than the theoretically predicted values. One of the reasons to account for is the transport effects of the cesium plasma.

The major types of transport effects are electron scattering and electron space charge. The effect of electron scattering attributing losses seems to be related to the resistivity of the cesium plasma. The effects of electron space charge are reduced or eliminated by positive ions, which are produced from the electrically supported ionization process. The latter is called ion generation losses. As a diagnosis tool, efforts were made trying to separate these losses. Typical work was the transient experiment reported by Kaplan (1).

Kaplan made a series of experiments in which potential or current pulses are applied to a cesium plasma diode. It was observed that the characteristics obtained are somewhat different than that of the steady state operation. This seems related to the transient response of the cesium plasma. Therefore, the purpose of this dissertation is to review the theoretical analysis that may apply to the transient or non-linear properties of the cesium plasma cell.

A. V-I Characteristics of the Diode

The V-I curves of typical cesium diodes are shown in Figure 1. The dashed line represents idealized condition, in which the saturation cur-

rent density J_s is from the Richardson's equation:

$$J_s = 120\ T_E^2 \exp\ (-\phi_{E/t_E}) \qquad (1)$$

where T_E and ϕ_E are emitter temperature and emitter work function, respectively. t_E is defined as $kT_{E/e} = T_{E/11,610}$ in which k is the Boltzmann constant and e is the electron charge.

The retarding portion of this curve (i.e. $\phi_E < \phi_C + V_0$) is the Boltzmann line, which is given by the emission equation:

$$J_0 = 120\ T_E^2 \exp\ (-V_{b/t_E}) - J_1 \qquad (2)$$

where J_0 is the output current, V_0 is the output voltage, V_b denotes emitter barrier voltage (Figure 2a) and J_1 represents no-load ion current.

The practical V-I curves are much lower than the ideal case. Furthermore, for higher loads the current density becomes double-valued known as the extinguished mode and the ignited mode. The ignited mode may be obtained after biasing the diode with external sources. The above mentioned characteristics are well known in steady state operation (2a). In Kaplan's experiments the curve recorded after pulsed discharge is, for some part, in good agreement with the Boltzmann's line.

Kaplan's curves may be called transient curves which are measured immediately after the pulsed discharge. As shown in Figure 1, the steady-state curve differs from the transient curves by a potential difference V_2, the voltage loss due to ion generation. At higher output current, the transient curve differs from the Boltzmann's line by a potential difference V_1, the voltage loss due to plasma resistance. Some calculations based on

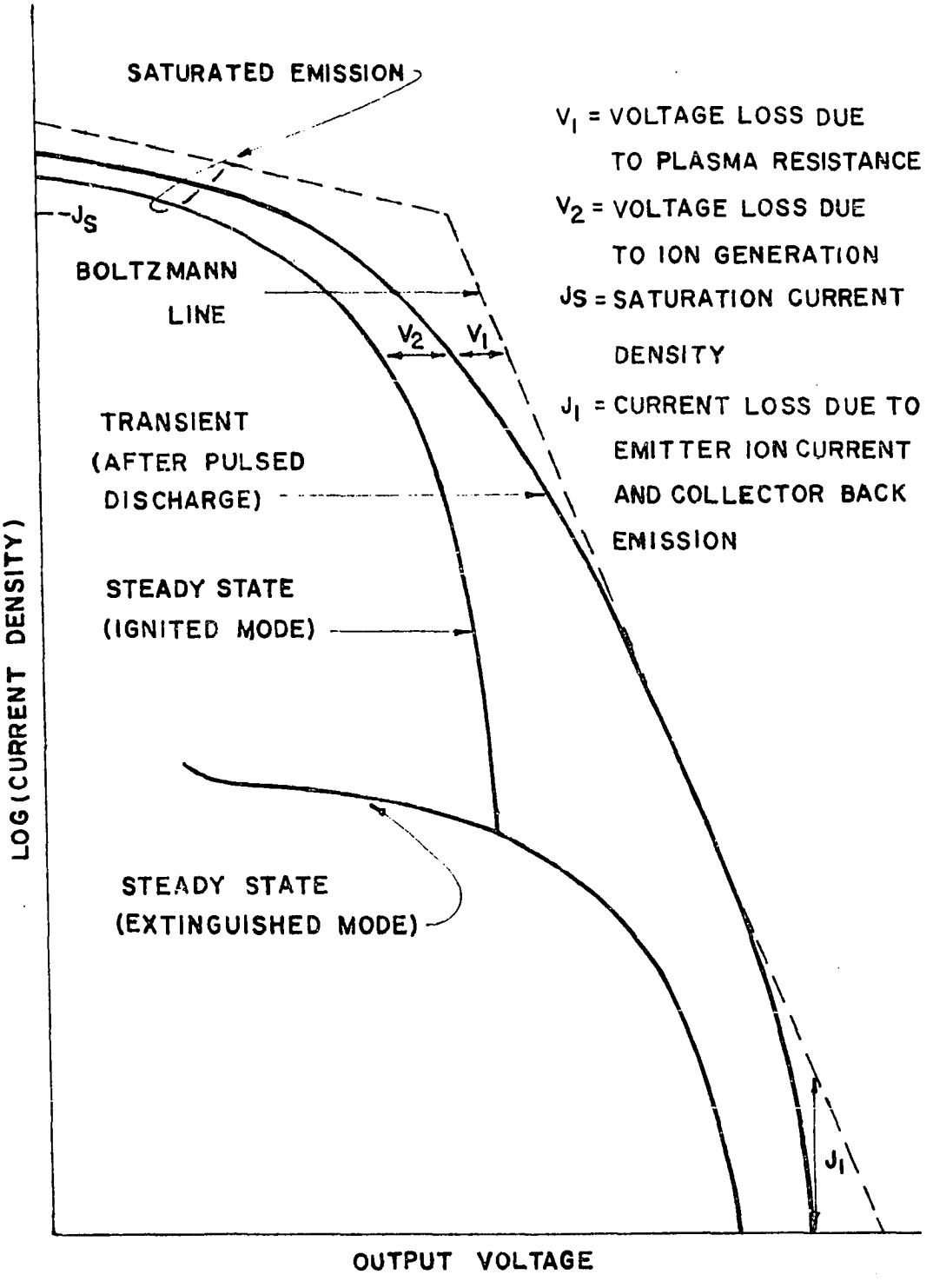

FIGURE I. TYPICAL STEADY-STATE AND TRANSIENT CURRENT-VOLTAGE CURVES

these curves are given in Part III, and the curves are compiled in the Appendix.

B. Potential diagrams in the diode space

Figure 2 illustrates the simplified potential diagrams of a plasma diode. Figure 2a is operated at low current extinguished mode. It is characterized by space charge limited in the diode space, and ions are generated by surface ionization. V_b is the barrier voltage that causes the low current capability. Figure 2b is the high current ignited mode. In this case, ions are produced by volume ionization, i.e. ionization by collision. Thus V_1 and V_2 are voltage losses due to ion generation and plasma resistance, respectively. At low output currents, excess of ions may exist in the plasma and the potential is represented by the dashed curve.

Figure 2c is the potential diagram after the pulsed discharge. In this case ions are generated by pulsing the diode with an external source thus $V_2 = 0$.

The theory and evidence of the foregoing phenomena which is closely related to the behavior of the cesium plasma, will be introduced in Part II.

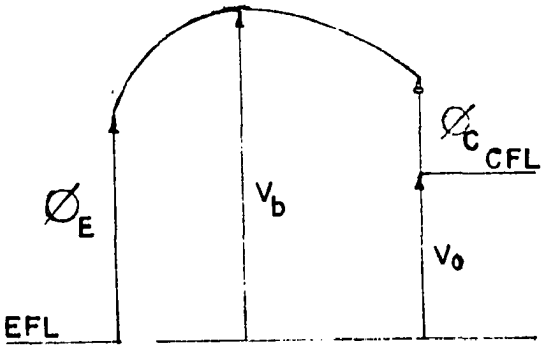

FIGURE 2A

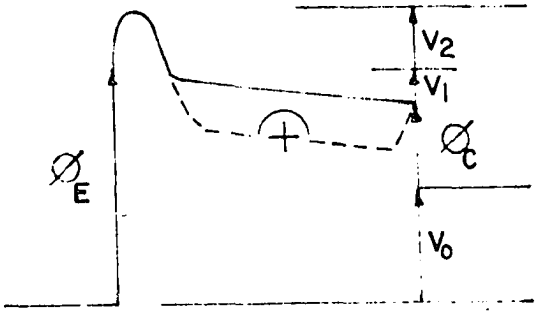

FIGURE 2B

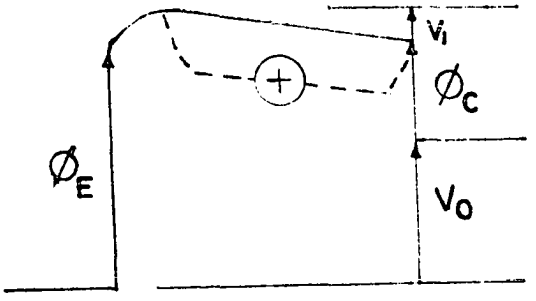

FIGURE 2C

LEGEND

EFL — EMITTER FERMI LEVEL

CFL — COLLETOR FERMI LEVEL

ϕ — WORK FUNCTION

V_b — EMITTER BARRIER VOLTAGE

V_o — OUTPUT VOLTAGE

V_1 — VOLTAGE LOSS DUE TO PLASMA RESISTANCE

V_2 — VOLTAGE LOSS DUE TO ION GENERATION

⊕ — EXCESS POSITIVE IONS

FIGURE 2. POTENTIAL DIAGRAMS OF THE DIODE

II. Macroscopic Behavior of The Cesium Plasma

A. Plasma Sheaths

For any bounded plasma there exists a sheath between the plasma and its confinement. The sheath serves as a barrier beyond which electric neutrality is maintained on both sides. In general voltage gradient and temperature gradient exist in the sheath. In some operating conditions of a thermionic converter these gradients may be very high. Here we shall investigate the electrical properties of the sheath from a very simple picture (Figure 3). Consider the sheath near the envelope which would be electron rich since electrons having higher velocity tend to escape from the plasma. Thus, it has been shown by Spitzer (2b), that the sheath thickness is in the order of Debye shielding distance.

1. Debye shielding distance

Let us consider a two-dimension case where the electric field E is parallel to the x axis. To derive the Debye shielding distance, we have from the one dimensional Poisson's equation

$$\frac{d^2V}{dx^2} = - \frac{q}{\epsilon_o} \tag{3}$$

where V is the electrical potential, q is the electric charge and ϵ_o denotes the permittivity of free space.

Consider a certain region with electron density n_e and ions may be neglected. Thus

$$\frac{d^2V}{dx^2} = \frac{n_e e}{\epsilon_o} \tag{4}$$

where e is the charge of electron.

If W denotes the potential energy of an electron, equals to -eV, then the change of W across a slab of width x is

$$\Delta W = - eV = \frac{-n_e e^2 x^2}{2}$$

provided

$$E = \frac{dV}{dx} = 0 \text{ at } x = 0.$$

The Debye shielding distance h is the value of x for which the absolute value of ΔW equals to $\frac{1}{2}kT_e$, the mean kinetic energy per particle in one direction. Therefore

$$h = \sqrt{\frac{\epsilon_o k T_e}{n_e e^2}} = 6.90 \sqrt{\frac{T_e}{n_e}} \quad \text{cm} \tag{5}$$

where k is the Boltzmann constant, T_e the kinetic temperature of the electrons in ^oK and n_e the electron density in cm^3.

2. Emitter sheath

The emitter sheath needed special attention in that it emitts electrons thermionically.

Let us choose a plane emitter at x = 0, and consider the region

$$0 \leq x \leq h,$$

We have, from equation (3)

$$\frac{d^2V}{dx^2} = \frac{e(n_e - n_i)}{\epsilon_o}$$

where $q = e (n_i - n_e)$, and n_i is the ion density.

The equation of motion for an electron in the x direction is

$$m_e \frac{dv_e}{dt} = e \frac{dV}{dx}$$

for $x < h$

assume $v_e = \sqrt{\frac{2eV}{m_e}}$

where v_e is the electron velocity and m_e is mass of the electron.

The current density is given by

$$J = e\,(n_i\, v_i - n_e\, v_e)$$

Since $v_i < v_e$, and $n_i << n_e$ when $x < h$

we have $J \approx - q\, v_e$

or $$q \approx - \frac{J}{v_e} \approx - \sqrt{\frac{m_e}{2eV}}$$

Therefore $$\frac{d^2V}{dx^2} = \frac{J}{\epsilon_o} \sqrt{\frac{m_e}{2eV}}$$

or $$\frac{d^2V}{dx^2} = C_1\, V^{-\frac{1}{2}} \qquad (9)$$

where $$C_1 = \frac{J}{\epsilon_o} \sqrt{\frac{m_e}{2e}}$$

Multiply equation (9) by $2\,(\frac{dV}{dx})$

$$2(\frac{dV}{dx})\ (\frac{d^2V}{dx^2}) = 2C_1\, V^{-\frac{1}{2}}\ \frac{dV}{dx}$$

Integrating $$(\frac{dV}{dx})^2 = 4C_1\, V^{\frac{1}{2}} + C_2$$

Since $$\frac{dV}{dx} = - E(x)$$

Let $E(0) = 0$ and $V(0) = 0$, then $C_2 = 0$

Thus $$\frac{dV}{dx} = 2\sqrt{C_1}\ V^{\frac{1}{4}}$$

Integrating again, we have

$$(4/3)\, V_s^{3/4} = 2\sqrt{C_1}\ X_s$$

where X_s is the sheath thickness and V_s is the sheath voltage. Finally by eliminating C_1,

$$X_s^2 = \frac{4\epsilon_o}{9}\sqrt{\frac{2e}{m_e}}\ \frac{V_s^{3/2}}{J}$$

or for the emitter sheath

$$X_{sE}^2 = 2.34 \times 10^{-6}\ \frac{(V_{sE})^{3/2}}{J_e} \qquad (10)$$

This equation is an application of Child's Law (3), in which X_{sE} denotes the emitter sheath thickness in cm, V_{sE} is the emitter sheath voltage in volts and J_e is the electron current density in amperes per cm^2.

Since the sheath thickness is in the order of Debye shielding distance, one can see from equation (10) that the emitter sheath voltage V_{sE} reaches its lowest value at open circuit ($J_e \approx J_o = 0$) and reaches its highest value near short circuit ($J_e \approx J_o = J_s$) conditions. Child's Law though simple and crude, gives the relation between the sheath thickness with its voltage and current. More detailed treatment by Taalat yields essentially the same conclusion (4).

3. Collector sheath

Similar argument in previous section is applied to the collector sheath. Consider an isolated collector with back emission current J_{eb},

the collector sheath thickness is given by the equation

$$X_{xC}^2 = 2.34 \times 10^{-6} \frac{(V_{sC})^{3/2}}{J_{eb}}$$

Since

$$\frac{J_{eb}}{J_{io}} = \sqrt{\frac{m_i}{m_e}} \tag{11}$$

as based on Langmiur's theory (5), where $\sqrt{m_{i/m_e}} = 492$ is the square root of mass of a cesium ion to mass of an electron; and J_{io} is the no load ion current at the collector sheath

Thus $$X_{sC}^2 = 2.34 \times 10^{-6} \sqrt{\frac{m_e}{m_i}} \frac{(V_{sC})^{3/2}}{J_{io}}$$

or $$X_{sC}^2 = 4.76 \times 10^{-9} \frac{(V_{sC})^{3/2}}{J_{io}} \tag{12}$$

During the diode operation, the collector sheath voltage reaches its highest value at open circuit ($J_{io} = J_{eo}$) and its lowest value near short circuited conditions ($J_i \approx 0$).

Figure 3 depicts the sheath voltages and currents of a diode carrying external loads. As mentioned previously, the potential at the edge of the plasma is positive with respect to that of both the emitter and the collector. Double sheaths are formed on the emitter surface due to the thermionic emission.

B. Plasma resistance

The plasma in a thermionic energy converter can be classified as low temperature or low energy ionized gas. The electrical conductivity of such an ionized gas was calculated by Cohen et al (6), in which two-body

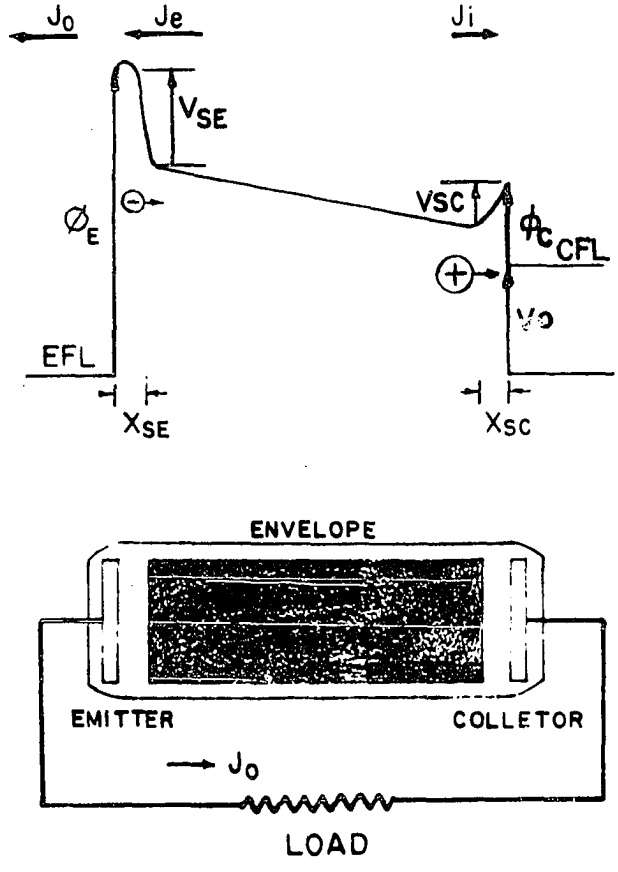

FIGURE 3. THE EMITTER AND COLLECTOR SHEATHS

interactions are considered among the ion-electron and electron-electron encounters. This is so called Coulombic scattering. The formation of the equations for calculation is given as below:

1. The Coulombic scattering

The velocity distribution function f_r (x, v, t) of type r, interacting with particles of different types s, is given by Boltzmann's equation:

$$\frac{\partial f_r}{\partial t} + \Sigma_i v_{ri} \frac{\partial f_r}{\partial x_i} + \Sigma_i F_{ri} \frac{\partial f_r}{\partial v_{ri}} = \Sigma_s \left(\frac{\partial_e f_r}{\partial t}\right)_s \qquad (13)$$

where v_{ri} is the component of velocity vector of an r-th particle in direction i, x_i is the component of position vector in direction i and F_{ri} is force per unit mass on particle of type r. $\left(\frac{\partial_e f_r}{\partial t}\right)_s$ denotes the change in f_r produced by encounters of r particles with particles of type s.

The right hand side of equation (13) is evaluated for inverse-square forces.

$$\left(\partial_e f_r/\partial t\right)_s = - J (f_r f_s) - K (f_r f_s) \qquad (14)$$

where $J (f_r f_s)$ is the close encounter function (5) defined as

$$J(f_r f_s) = \int_{v_s = 0}^{\infty} \int_{\epsilon = 0}^{2\pi} \int_{b = 0}^{b_c} (f_r f_s - f_{r'} f_{s'}) \, gbdbd\epsilon d\bar{v}_s \qquad (15)$$

in which $f_{r'}$ is the velocity distribution function after collision, $g = \bar{v}_r - \bar{v}_s$ the relative velocity of the two types of particle before encounter, b is the impact parameter, ϵ is the angle between the orbital plane and the plane containing the velocities of the two particles before

encounter; and b_c represents the critical impact parameter.

$K(f_r f_s)$ is the distant encounter function defined as

$$K(f_r f_s) = \Sigma_i \frac{\partial}{\partial v_i} (f_r < \Delta v_{i,s} >) - \frac{1}{2} \Sigma_{i,j} \frac{\partial^2}{\partial v_i \partial v_j} (f_r < \Delta v_{i,s} \Delta v_{j,s} >) \tag{16}$$

where, in general, for any quantity x.

$$< x_s > = \int_{v_{s=0}}^{\infty} g f_s \, dv_s \int_{\epsilon=0}^{2\pi} d\epsilon \int_{b=b_c}^{b_m} x b db \tag{17}$$

in which b_c is the cut-off impact parameter. The higher ordered terms of $K(f_r f_s)$ in equation (16) are neglected. To solve for f_r, one would substitute equations (14), (15) and (16) into (1). It is a matter of complexity to solve these equations. Here we shall give some important steps that would lead to the equation for evaluating the conductivity.

According to Chapman and Cowling (7), let

$$f_r = f_r^{(0)} + f_r^{(1)} \tag{18}$$

where $f_r^{(0)}$ is the Maxwellian velocity distribution function. In equation (1), for a plasma in steady state with an electric field E and temperature gradient ∇T, it can be shown that

$$f_r^{(0)} \left\{ \frac{m_r v_r^2}{2kT} - \frac{5}{2} \right\} \Sigma_i v_{ri} \frac{\partial T}{T \partial x_i} - f_r^{(0)} \frac{eZ_r}{kT} \Sigma_i E_i v_{ri}$$

$$+ \Sigma_s K(f_r^{(1)} f_s^{(0)}) + \Sigma_s K(f_r^{(0)} f_s^{(1)}) = 0 \tag{19}$$

where Z_r equals to -1 for electrons. When equation (19) is applied to an

electron gas, we shall omit all subscripts from quantities referring to electrons, such as $f^{(0)}$, $f^{(1)}$, m and v.

For a more simple case, let $\nabla T = 0$ and define

$$\ell^2 = m/2kT$$

Thus
$$(2 \ell^2 ef^{(0)}/m) \Sigma_i E_i v_i + \Sigma_s K (f^{(1)} f_s^{(0)}) + \Sigma_s K (f^{(0)} f_s^{(1)}) = 0 \qquad (20)$$

The value of $f^{(0)}$ and $f^{(1)}$ may be represented in spherical coordinates.

$$f^{(1)} (\bar{v}) = f^{(0)} D (\ell v) \cos \theta \qquad (21)$$

where D is the diffusion function, θ is the angle between $\bar{E}$ and $\bar{v}$, and $f^{(0)}$ is the Maxwellian distribution function, given by the equation

$$f^{(0)} (v) = (n_e \ell^3/\pi^{3/2}) \exp (- \ell^2 v^2) \qquad (22)$$

Thus, for an electron-proton gas equation (20) becomes

$$(2 \ell^2 ef^{(0)}/m) E v \cos \theta + K (ff_p) + K (ff) = 0 \qquad (23)$$

where $K (ff_p)$ may be evaluated from equations (16) and (21), after transformed to spherical coordinates, we have,

$$K(ff_p) = [3Lf^{(0)} D (\ell v) \cos \theta]/2v^3 \qquad (24)$$

in which

$$L = (8 \pi e^4 n_e/3m^2) \ln (h/b_o)$$

where h is the Debye shielding distance and b_o is the impact parameter corresponding to 90^o deflection. h and b_o are the upper and lower limits, respectively, in evaluating $\langle x_s \rangle$ in equation (17). They are given by the equation

$$\frac{h}{b_o} = \frac{3}{Z_p e^3} \left(\frac{k^3 T^3}{\pi n_e}\right)^{\frac{1}{2}} \tag{25}$$

where Z_p is the charge of the ion.

Substituting equation (24) into equation (23), one finds the relation between $D(\ell v)$ and E is given by:

$$(2\ell^2 \, ef^{(0)}/m) \, Ev \cos\theta + (3Lf^{(0)} \, D(\ell v) \cos\theta)/2v^3 + K(ff) = 0 \tag{26}$$

Multiply equation (26) by $\left(2\pi v^3 \cos\theta \sin\theta \, dv \, d\theta\right)$ and integrate over all θ and v; letting $x = \ell v$, and define

$$I_n(\infty) = \int_0^\infty y^n D(y) \exp(-y^2) \, dy \tag{27}$$

Thus $$I_0(\infty) = \int_0^\infty D(x) \exp(-x^2) \, dx = \frac{3\pi^{\frac{1}{2}} A}{8}$$

Where $$A = -\frac{mE}{2\pi \ell^2 e^3 n_e \ln(h/b_o)} \tag{28}$$

The integration of K(ff) in equation (26) dropped out since the electron-electron intractions can not change the total momentum of the electrons. Finally, the conductivity is given by the equation

$$\sigma = \int_{v=0}^{\infty} \int_{\phi=0}^{2\pi} \int_{\theta=0}^{\pi} \frac{-f(v)\ ev\ \cos\theta}{E}\ v^2 \sin\theta\ d\theta\ d\phi\ dv \tag{29}$$

Substitute equations (18), (21) and (22) into equation (29) and integrating, the $f^{(0)}$ term vanishes because of spherical symmetry.

Thus
$$\sigma = \int_{v=0}^{\infty} \int_{\phi=0}^{2\pi} \int_{\theta=0}^{\pi} \frac{f^{(0)}(v)\ D(\ell v)}{E}\ v^3 e\ \cos^2\theta\ d(\cos\theta)\ d\phi\ dv$$

$$= \frac{2}{3} \cdot 2\pi \int_{\ell v=0}^{\infty} \frac{n_e\ e^3 v^3\ D(\ell v)\ \exp(-\ell^2 v^2)\ d(\ell v)}{\pi^{3/2} E \ell}$$

$$= \frac{4\pi e n_e}{3E\ell} \int_{y=0}^{\infty} y^3\ D(y)\ \exp(-y^2)\ dy$$

$$= \frac{4\pi e n_e}{3E\ell}\ I_3(\infty) \tag{30}$$

where $I_3(\infty)$ is defined by equation (27).

Combining equations (28) and (30), we have

$$\sigma = \frac{2m\ I_3(\infty)}{3\ell^2 e^2 \pi^{3/2} A\ \ln(h/b_o)}$$

For Lorentz gas, a fully ionized gas in which the electrons do not interact with each other and the ions are at rest,

$$\frac{I_3(\infty)}{A} = 3$$

Let $$\gamma = \frac{I_3(\infty)}{3A}$$

Thus $$\sigma = \frac{2m\gamma}{3e^2\pi^{3/2}\ln(h/b_o)}$$

For singly charged ions $\gamma = 0.58$ (2), therefore, the final equation of resistivity is given by

$$\rho = \frac{\pi^{3/2}\, m^{\frac{1}{2}}\, e^2 \ln(h/b_o)}{2(0.58)\,(2kT)^{3/2}}$$

$$= 6.53 \times 10^3 \; \frac{\ln\Lambda}{T^{3/2}} \text{ ohm-cm} \qquad (31)$$

where $$\Lambda = h/b_o$$

Equation (31) is the Spitzer-Härm formula for resistivity of plasma. It is well accepted in the field of plasma physics for a weakly external field E and at temperature T not too high. These conditions apply to the cesium plasma inside a thermionic energy converter. However, one should realize that the temperature gradient ∇ T which was omitted in equation (20) does exist in an energy converter, and the temperature T in equation (31) is the mean kinetic temperature of the electrons in the plasma.

2. The electron-neutral scattering

The contribution of the collisions between electrons and neutrals would highly depend on the external sources, since there is no interaction force between electrons and neutrals. Furthermore, one would suspect that there would be a collision cross section involved in the process. In the following derivation, we shall adopt the Robinson's model (8), that in a homogeneous plasma there is an external field $E(t)$ in the x direction. Again, we may write Boltzmann's equation

$$\frac{\partial f_e(\bar{v}_e,t)}{\partial t} + \frac{eE(t)}{m_e} \frac{\partial_e(\bar{v}_e,t)}{\partial v_{ex}} = \left(\frac{\partial f_e(\bar{v}_e,t)}{\partial t}\right)_c \tag{32}$$

when collisions between electrons and neutral atoms are the only type of importance, the right hand side of equation (32) becomes

$$\left(\frac{\partial f_e}{\partial t}\right)_c = \int_{\bar{v}_e=0}^{\infty} \int_{Q=0}^{Q_m} g\, dQ \left[f'_e f'_o - f_e f_o\right] d\bar{v}_e \tag{33}$$

where the subscript e denotes electrons and o denotes neutrals, (from now on we shall drop the e's for the electrons), f, f', g and $\bar{v}$ are defined as in equation (15). Note that equation (33) is written in closed form as distant encounters are neglected. dQ is the scattering cross section defined by

$$dQ = I(v,\chi)\, d\Omega$$

where $d\Omega = \sin x\, dx\, d\epsilon$ in which χ is the deflection angle and ϵ is the polar angle. $I(v,\chi)$ is the differential cross-section given by the equation

$$I(v,\chi) = \frac{1}{4K^2}\left\{ \sum_{\ell=0}^{\infty} (2\ell + 1) [\exp (2_j \delta_\ell) - 1] P_l(\cos\chi) \right\}^2$$

where $K = mv/\hbar$, δ_ℓ is the l-th order phase shift and $P_l(\cos\chi)$ is the ℓ-th order Legendre's polynomial.

After some simplifications, equation (32) is reduced to

$$\frac{d < v_x >}{dt} + N_o \int f\, v_x\, vQ_M(v)\, d\bar{v} = \frac{eE(t)}{m_e} \tag{34}$$

where $< v_x >$ is the average speed of electrons defined by

$$< v_x > = \int f(v,t)\, v_x\, d\bar{v}$$

N_o is the number of neutral particles per cm^3 and $Q_M(v)$ is the momentum transfer cross-section. In most cases, $Q_M(v) \propto 1/v$ i.e. the momentum transfer function is proportional to the inverse of the relative speed between the two particles. Thus one finds equation (32) in a very familiar form

$$\frac{d <v_x>}{dt} + \mu <v_x> = \frac{eE(t)}{m_e} \tag{35}$$

where μ is the collision frequency defined by

$$\mu = \int N_o\, vQ_M(v)\, d\bar{v}$$

Let ρ_n be the plasma resistivity resulting from electron-neutral collisions, and since

$$J_n = E/\rho_n$$

and
$$J_n = n_e\, e\, \langle v_{ix} \rangle \tag{37}$$

Assuming $E(t) = E_x \exp(j\omega t)$

then
$$\langle v_x \rangle = \frac{e}{m_e} \frac{E_x \exp(j\omega t)}{\mu + j\omega} \tag{38}$$

Therefore, at low frequencies

$$\rho_n = \frac{m_e \bar{\mu}}{n_e e^2} \tag{39}$$

or
$$\rho_n = \frac{N_o m_e \bar{\mu}_1}{n_e e^2} \tag{40}$$

where $\bar{\mu}_1$ represents the average collision frequency per neutral atom and is given by

$$\bar{\mu}_1 = 2\pi \int_{\bar{v}=0}^{\infty} \int_{x=0}^{\pi} f(\bar{v})\, vI(v,\chi)\, (1 - \cos\chi)\, \sin\chi d\chi d\, \bar{v}$$

where $\bar{\mu} = N_o \bar{\mu}_1$. For $f(\bar{v})$ in Maxwell-Boltzmann distribution, the values of μ have been calculated by Robinson and others (8). It was shown $\bar{\mu}$ depends weakly on temperature. At high temperature, $\bar{\mu}$ approaches to 10×10^{-7} cm^3 sec^{-1} and $\bar{\mu} \approx 9 \times 10^{-7}$ cm^3 sec^{-1} for the range of thermionic energy converters (2000°K).

Defining the fractional of ionization $f_s = n_e/(N_o + n_e)$, equation (40) can be written as

$$\rho_n = 3.57 \times 10^3 \bar{\mu} \left(\frac{1-f_s}{f_s}\right) \tag{41}$$

where f_s may be obtained from Nottingham's theory on fractional ionization (9)

$$f_s = 1 - \frac{1.9 \times 10^{-6} \sqrt{T_{Cs}} \; \mathrm{esp}\left(\frac{V_i}{t_e}\right)}{(t_e)^{3/2} \left(2 + \frac{V_i}{t_e}\right)}$$

in which V_i is cesium first ionization potential and equals 3.87 volts, t_e is the electron temperature in equivalent volts, i.e. $t_e = T_e/11{,}610$ volts as defined previously.

The fractional ionization can also be obtained by using a Langmuir probe to measure the electron density in the plasma.

C. Plasma reactance

It was reported by Firle (10) and Laubenstein et al. (11), that the current decay time after a pulsed discharge is in the order of 100 microseconds. In addition, their results indicate that the decay time is not sensitive to electrode spacing, cesium pressure and other parameters. This phenomenon can be described by attributing the property of inductances to the plasma. On the other hand, plasma oscillations are well known at high frequencies. It follows that the electric circuit and electromagnetic field analogy may be applied to the plasma at lower frequencies and higher frequencies, respectively. The concept of plasma reactance is treated in the following two sections.

1. Low frequency inductive reactance

Referring to equation (35), one can substitute $< v_x >$ with J_n and obtain the following equation

$$\frac{dJ_n}{dt} + \mu(t) J_n = \frac{n_e e^2 E(t)}{m} \tag{42}$$

where J_n is the current density attributing to electron-neutral scattering. $\mu(t)$ represents the collision frequency which in general is time dependent as can be seen from the defining equation

$$\mu(t) = N_o(t) \, v Q_M(v) \, f(v,t) \, dv \tag{43}$$

In which the density of neutral cesium atoms $N_o(t)$ is time dependent during the discharge and the velocity distribution function $f(v,t)$ would naturally depend on time during the transient process. However, for the sake of simplicity, we shall assume that they would stay at their initial values during the current decay or the current build up process.

Thus the time constant is given by

$$\tau = \frac{1}{\mu} = \frac{1}{N_o \bar{\mu}_1} \tag{44}$$

where $\bar{\mu}_1 = 9 \times 10^{-7}$ cm^3/sec for the temperature range of interest.

As mentioned previously, the measured current "decay" time constant after a pulsed discharge is approximately 100 microseconds, so let $\tau = 100 \times 10^{-6}$ second and check if other conditions are satisfied. From equation (44) the number of neutral cesium atoms per cm^3 is

$$N_o = \frac{1}{10^{-4} \times 9 \times 10^{-7}} = \frac{10^{11}}{9} = 1.11 \times 10^{10} \text{ neutrals/}_{cm^3}$$

For cesium vapor pressure P = 0.2 mm Hg, cesium temperature $T_{Cs} = 300^{o}C$, the corresponding gas molecule density $N_g = 2.76 \times 10^{15}$ molecules/$_{cm^3}$

Thus the fraction of ionization

$$f_s = 1 - \frac{N_o}{N_g} = 1 - 4 \times 10^{-6} \approx 1$$

which means the gas is fully ionized.

During the positive pulse is applied to the diode, the current build up is much faster then that of the decay. This is because of low fractional ionization at the extinguished mode. Typical "rising" time constant may be calculated very briefly: For cesium pressure P = 0.2 mm H_g, $T_{Cs} = 300^{o}$ C $N_o \approx N_g = 2.76 \times 10^{15}$ neutrals/$_{cm^3}$

Thus $$\tau = \frac{1}{N_o \bar{\mu}_1} = \frac{1}{2.76 \times 10^{15} \times 9 \times 10^{-7}} = 4 \times 10^{-9} \text{ sec}$$

In the case when a positive pulse is applied to a diode already at ignited mode (Fully ionized), $\mu(t)$ would depend strongly on $E(t)$ in equation (42) and the situation is better dipited by Coulombic scattering in section II - B - 1.

The above discussion is based on the assumption that the current decay is exclusively due to electron-neutral collisions. Similar argument

may be applied to the charge exchange collision in which cesium ions collide with cesium atoms. Sheldon (12) calculated the average momentum-exchange cross-section for charge exchange collisions $\bar{Q}_{ce} = 5.0 \times 10^{-13}$ cm^2 at cesium temperature of 300°K, as compared to $\bar{Q}_{en} = 5.0 \times 10^{-14}$ cm^2 for electron-neutral collisions at the same temperature (8). Accordingly, one can compute the charge exchange collision frequency from equation (43). Realizing that the average cesium ion speed is approximately 1/492 that of the electrons and assuming the cesium ions have the same distribution function as the electrons, we have obviously,

$$\mu_{ce} = \frac{7 \times 10^{-7} \times 2 \times 10^{-13}}{492 \times 5 \times 10^{-14}} = 5.7 \times 10^{-9} \text{ cm}^3/\text{sec at } 300^\circ\text{K}$$

2. High frequency capacitive reactance

When a high frequency e.m.f. is applied to a cesium plasma thermionic diode, the latter reacts more like a perturbed resonant cavity. In effect, the diode can support several different kinds of oscillations corresponding to different modes of operation in resonant cavities (13). Shure (14) has treated the plasma oscillation as boundary value problems and derived an equation for the plasma capacitor. His simplified and generalized analysis though may not apply to the cesium diode in some respects, but it does give the insight as to the problems involved. Thus we shall begin with the assumptions and hopefully conclude to a useful result.

The starting point is the Vlasov "collisionless" Boltzmann equation and the Poisson equation. We shall consider a plasma-filled parallel plate capacitor as shown in Figure 4. An e.m.f. of frequency ω is imposed upon the electrodes. The coupled one-dimensional Vlasov and Poisson

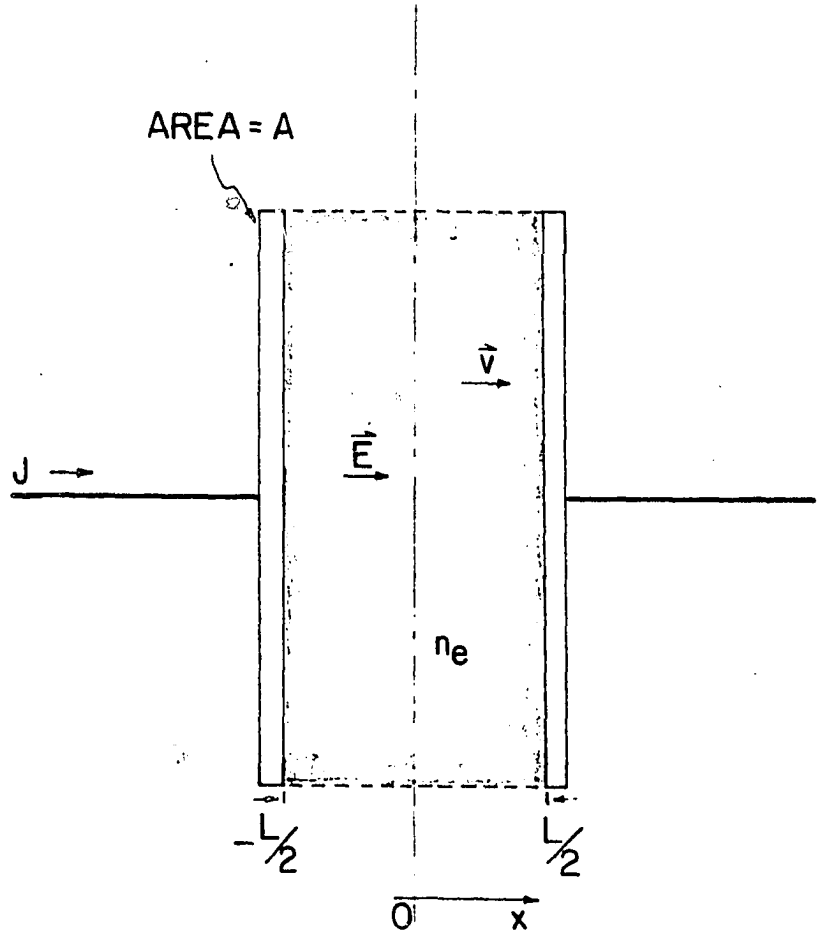

FIGURE 4. SIMPLE GEOMETRY FOR CALCULATING PLASMA CAPACITANCE

equations are

$$\frac{\partial}{\partial t} f(x,v,t) + v \frac{\partial f}{\partial x} = - \frac{n_e e}{m} E(x,t) \frac{dF(v)}{dv} \tag{44}$$

$$\frac{\partial}{\partial x} E(x,t) = 4\pi e \int_{-\infty}^{\infty} f dv \tag{45}$$

The Vlasov equation has been linearized about its equilibrium solution

$$\mathcal{F}(x,v,t) = n_e F(v) + f(x,v,t) \tag{46}$$

where $F(v)$ is the Maxwellian distribution function at temperature Ω/k. The variables x, v, t may be replaced with the following non-dimensional parameters

$$x' = \frac{x}{h} \qquad v' = \frac{v}{h\omega_p} \qquad t' = t\omega_p \tag{47}$$

where h is the Debye shielding distance and ω_p is the plasma frequency given by the equations

$$h^2 = \frac{\Omega}{4\pi n_e e^2} \qquad \omega_p^2 = \frac{4\pi n_e e^2}{m} \tag{48}$$

In addition, the frequency of the impressed field is in terms of ω_p such that

$$\omega' = \omega/\omega_p$$

Substitute these new variables in equations (44) and (45) and subsequently

drop all the primes

$$\frac{\partial f}{\partial t} + v \frac{\partial f}{\partial x} = \frac{-1}{4\pi} \frac{dF(v)}{dv} E \tag{50}$$

$$\frac{\partial E}{\partial x} = 4\pi \int_{-\infty}^{\infty} f(v,t)\, dv \tag{51}$$

$$F(v) = \frac{1}{\sqrt{2\pi}} \exp\left(-v^2/2\right) \tag{52}$$

We shall assume the system has time dependence exp $(-j\omega t)$, i.e.

$$E(t) = E \exp(-j\omega t).$$

The coupled equations may be represented by a single matrix equation

$$\begin{pmatrix} v & 0 \\ 0 & 1 \end{pmatrix} \frac{\partial}{\partial x} \begin{pmatrix} f \\ E \end{pmatrix} = \begin{pmatrix} j\omega & -\frac{1}{4\pi} \frac{dF}{dv} \\ 4\pi \int_{-\infty}^{\infty} & 0 \end{pmatrix} \begin{pmatrix} f \\ E \end{pmatrix} \tag{53}$$

or symbolically,

$$\rho \frac{\partial \psi}{\partial x} = H \psi \tag{54}$$

where ψ is the "state vector"

$$\psi = \begin{pmatrix} f \\ E \end{pmatrix} \tag{55}$$

The solutions of the integro-differential matrix equation depend on the eigen values of the characteristic function as well as the boundary conditions imposed. For our purpose $\omega \leq 1$ is the range of interest, this narrows down to the solutions of the so called discrete normal modes:

$$\psi = \psi_i \exp(j\omega x/\gamma_i) \tag{56}$$

$$f_i = \frac{\nu_i^2}{\omega^2} \frac{dF/dv}{v-\nu_i} \tag{57}$$

$$E_i = \frac{4\pi \nu_i}{j\omega} \tag{58}$$

The eigen values ν_i are the zeros of the characteristic function

$$\Lambda(\nu) = 1 - \frac{\nu^2}{\omega^2} \int_{-\infty}^{\infty} \frac{dF/dv}{v-\nu} \, dv \tag{59}$$

$\Lambda(\nu)$ is analytic in the complex ν-plane cut along the entire real axis, and tends to a constant value for large $|\nu|$

$$\Lambda(\infty) = 1 - \frac{1}{\omega^2} \tag{60}$$

For Maxwellian F(v) and in the range $\omega < 1$, it may be shown that there are two discrete roots: $\nu_\pm = \pm j \nu_o$ with ν_o real and positive. The value of ν_o is shown in Figure 5. As shown in the figure the ordinate $\nu_{o/\omega}$ indicates the sheath thickness. When $\omega \to 0$ the sheath thickness equals the Debye shielding distance and as $\omega \to 1$ the sheath thickness increases rapidly. When $\omega = 1$ the plasma is in oscillation so effectively the diode will draw saturation current (15). This agrees very well to the discussion in section II-A-1 on the emitter and collector sheaths.

To find the capacitance of the plasma, the electric field E(x) may be evaluated using the boundary condition

$$f(v, \pm L/2) = f(-v, \pm L/2) \tag{61}$$

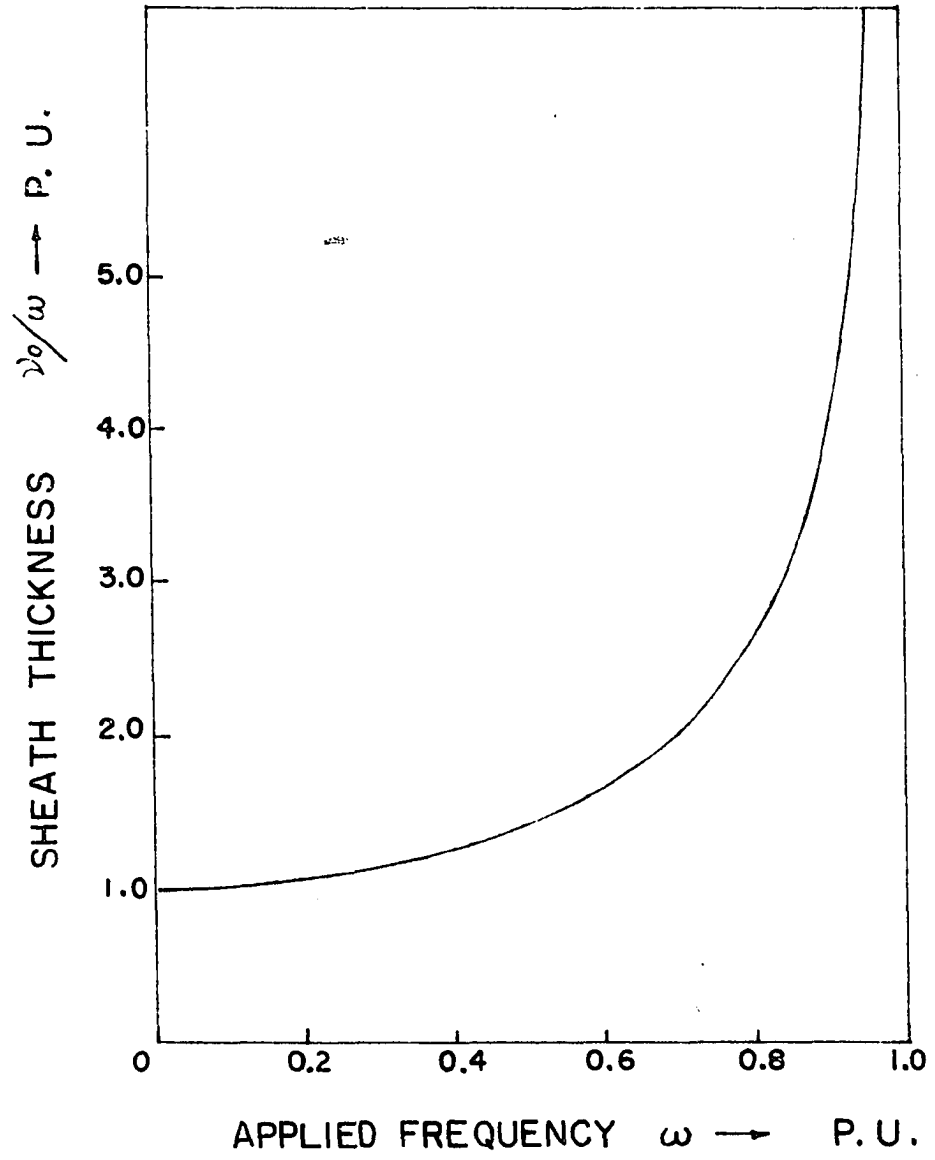

FIGURE 5. SHEATH THICKNESS VS. APPLIED FREQUENCY

and $$E\left(\frac{L}{2}\right) = - E(-L/_2) \tag{62}$$

The detailed derivation is omitted and finally for $\omega < 3/4$

$$E(x) \approx E\left(\frac{L}{2}\right) \left\{ 1 - \cosh\left[\frac{\omega}{\nu_o} x\right] \Big/ \cosh\left[\frac{\omega}{\nu_o} \frac{L}{2}\right] \right\} \tag{63}$$

The impedance Z of the capacitor is found from Ohm's law

$$ZJ = \int_{-L/_2}^{L/_2} E(x)\, dx \tag{64}$$

Substitute equation (63) in equation (64) and integrate

$$ZJ = E\left(\frac{L}{2}\right) \left\{ 1 - \frac{2}{L} \frac{\nu_o}{\omega} \tanh\left[\frac{\omega}{\nu_o} \frac{L}{2}\right] \right\} \tag{65}$$

Since J is the displacement current of the capacitor

$$\frac{J}{A} = \frac{j\,\omega}{4\,\pi} E\left(\frac{L}{2}\right) \tag{66}$$

A is the area of the plates

Thus $$Z = \frac{1}{j\,\omega\, C_o} \cdot \frac{1}{\epsilon_{eff}} \tag{67}$$

Where $$C_o = \frac{A}{4\,\pi\, L} \tag{68}$$

the capacitance of the condenser without the plasma, and the effective permittivity of the plasma is given by

$$\epsilon_{eff} = 1 - \frac{\tanh \frac{\omega}{\nu_o} \frac{L}{2}}{\frac{\omega}{\nu_o} \frac{L}{2}} \tag{69}$$

Hence the capacitance of a plasma condenser varies as the applied frequency ω. Its value depends on the sheath thickness $\lambda_{o/\omega}$ and thus in turn depending on the electron density n_e.

Furthermore, since $(\tanh x)/x$ approaches to unity when x is small, and approaches to zero when x is large, the effective permittivity ϵ_{eff} in equation (69) increases and approaches to 1, the permittivity of free space, as the spacing L increases. This is contradictory to conventional capacitors. However, the explanation stands by itself in that shorter spacing allows higher frequency oscillations supported by lower capacitance which is in fact experimentally proved by Rocard (16) for a low pressure plasma diode.

III. INTERPRETATION OF EXPERIMENTAL EVIDENCE

The theories developed in Part II are applied here to explain some experimental evidence reported elsewhere. In particular, some numerical results from Kaplan's transient experiments (1) is further calculated and his curves are compiled in the Appendix.

A. Experimental technique

The circuitry for transient measurements needed special attention in that stray pick up may highly effect the results. Coaxial cables can be used to reduce the circuit inductance. The external source to be applied to the diode should be carefully programmed and with negligible source impedance. The source that Kaplan used produces single pulses in the microsecond range with a current capability of 300 amperes. The switching circuit and its precise timing is of paramount importance. In the case alternating pulses are used, the linearity of coupling devices such as transformers must be concerned.

As for the diode converter itself, it is better to have parallel plate electrodes with adjustable spacing. A pot-window is necessary to view the discharge. The ultimate goal is to install Langmuir's probe that would reveal more precious information in the interelectrode space.

B. Calculations

1. Debye shielding distance

From equation (5), assume $T_e = 1573^{\circ}K$ and $n_e = 4 \times 10^{12}$ electrons/cm^3

$$h = \sqrt{\frac{\epsilon_o k T_e}{n_e e^2}} = \sqrt{\frac{1.38 \times 10^{-16} T_e}{4\pi \times 4.8 \times 10^{-10} n_e}}$$

$$= 6.9 \sqrt{\frac{T_e}{n_e}}$$

$$= 1.37 \times 10^{-4} \text{ cm.}$$

2. Collector sheath thickness at no load

Applying equation (12) and using the data from Figure 14, the collector sheath thickness at no load may be found. The no load ion current is J_1 as illustrated in Figure 1, thus $J_{io} = 0.056$ amp/cm^2. The collector sheath voltage is approximated by the potential difference between the transient curve and the Boltzmann's line, i.e. $V_{sc} = 0.22$ volts. Substituting in equation (12)

$$(X_{sc})^2 = 4.76 \times 10^{-9} \frac{(0.22)^{3/2}}{0.056}$$

therefore, $X_{sc} = 0.94 \times 10^{-4}$ cm

3. Emitter sheath voltage at near saturated current

From the result of equation (10), we shall assume the sheath thickness equals the Debye shielding distance, i.e. $X_{sE} = 1.4 \times 10^{-4}$ cm

Assume $J = 20$ amp/cm^2

Thus $(1.4 \times 10^{-4})^2 = 2.34 \times 10^{-6} \frac{(V_{sE})^{3/2}}{20}$

Therefore, $V_{sE} = 0.31$ volt

Similarly, the emitter sheath voltage is found to be 0.4 volt at an output current of 30 amperes. The voltage loss due to emitter sheath drop is appreciable at near-saturation current, and the diode is operated in the space charge limited region.

4. Plasma resistivity

From equation (31),

$$\rho = 6.53 \times 10^{3} \frac{\ln \Lambda}{T_E^{3/2}} \quad \text{ohm-cm}$$

where $$\Lambda = 1.24 \times 10^{4} \left(\frac{T_E^{3}}{n_e}\right)^{\frac{1}{2}}$$

Here the electron temperature is approximated by the emitter temperature, and the electron density is estimated by the equation

$$n_e = \frac{J_o}{e} \left(\frac{2 \pi m}{k T_E}\right)^{\frac{1}{2}} \tag{70}$$

The values based on Kaplan's experiments (1) are computed as follows:

For $J_o = 10$ amp/$_{cm^2}$ and $T_E = 1573^{o}K$. $n_e = 4 \times 10^{12}$ electrons/$_{cm^3}$ and $\ln \Lambda = 6.0$

Thus $\rho = 0.60$ ohm-cm for $T_E = 1350^{o}C$

and $\rho = 0.66$ ohm-cm for $T_E = 1250^{o}C$

The above calculated resistivity is checked against the measured resistivity, which is given by the equation

$$\rho = V_1/(J_o S) \tag{71}$$

where S is the spacing between the emitter and the collector, J_o is the output current and V_1 is the voltage loss due to plasma resistance (See Figure 1).

A plot of measured resistivity versus output current density is shown in Figure 6, for which the data are based on the transient curves in Figures 7 to 14 of the Appendix. The plot shows that the resistivity increases with higher cesium pressure but decreases with higher emitter temperature or higher current density. The higher resistivity at higher cesium pressures may be attributed to the electron-neutral scattering. The resistivity is inversely proportional to the emitter temperature as readily can be seen from equation (31). The dependence of resistivity on current, however, is uncertain due to a correction factor involved in the experiment*. It may be further noted that the current density plotted in Figure 6 is in the range of 5 to 15 amperes per sq. cm, at which the transport effect starts to play. For higher current near to saturation, the emitter sheath voltage should be considered in determining the voltage drop due to plasma resistance V_1.

5. Plasma inductance

The inductance of a plasma may be found from the relation $\tau = L/R$ where τ is given by equation (44). Thus for $\rho = 0.66$ ohm-cm, the emitter or collector area $A = 4.6$ cm^2 and the emitter and collector spacing $S = 0.038$ cm we have $R = \rho \frac{S}{A} = 5.45 \times 10^{-3}$ ohm

*Kaplan, Cole, Marquardt Corporation, Van Nuys, California. Experimental Techniques. Private communication. 1964.

Since $\tau = 10^{-4}$ sec

Hence $L = 5.45 \times 10^{-3} \times 10^{-4} = 5.45 \times 10^{-7}$ henry

This gives the order of magnitude of plasma inductance on the basis of electron-neutral scattering.

6. Plasma capacitance

Using the foregoing dimensions, the capacitance without plasma is obtained from equations (68) and (69):

$$C_o = \frac{A}{4\pi S} = \frac{4.6}{4\pi (0.038)} \times \frac{10^{-11}}{9} = 10.7 \times 10^{-12} \text{ farad}$$

The effective permittivity $\epsilon_{eff} = 1 - \dfrac{\tanh \frac{\omega}{\nu_o} \frac{L}{2}}{\frac{\omega}{\nu_o} \frac{L}{2}}$

Assuming $\dfrac{\omega}{\nu_o} \dfrac{L}{2} = \dfrac{0.38}{1.4 \times 10^{-4} \times 2} = 1360$

$$\left(\tanh \frac{\omega L}{\nu_o 2}\right) / \frac{\omega L}{\nu_o 2} = \frac{1}{1360}$$

Hence $\epsilon_{eff} = 1 - \dfrac{1}{1360} \approx 1$

Thus the plasma capacitance is equal to the electrode capacitance without plasma for the frequencies below the Langmuir frequency.

C. Discussion

It is well known that the dynamic behavior of ionized gases is a very complex problem. So far work has been done on simplified assumptions such as equilibrium state, linearized variations and other negligible effects.

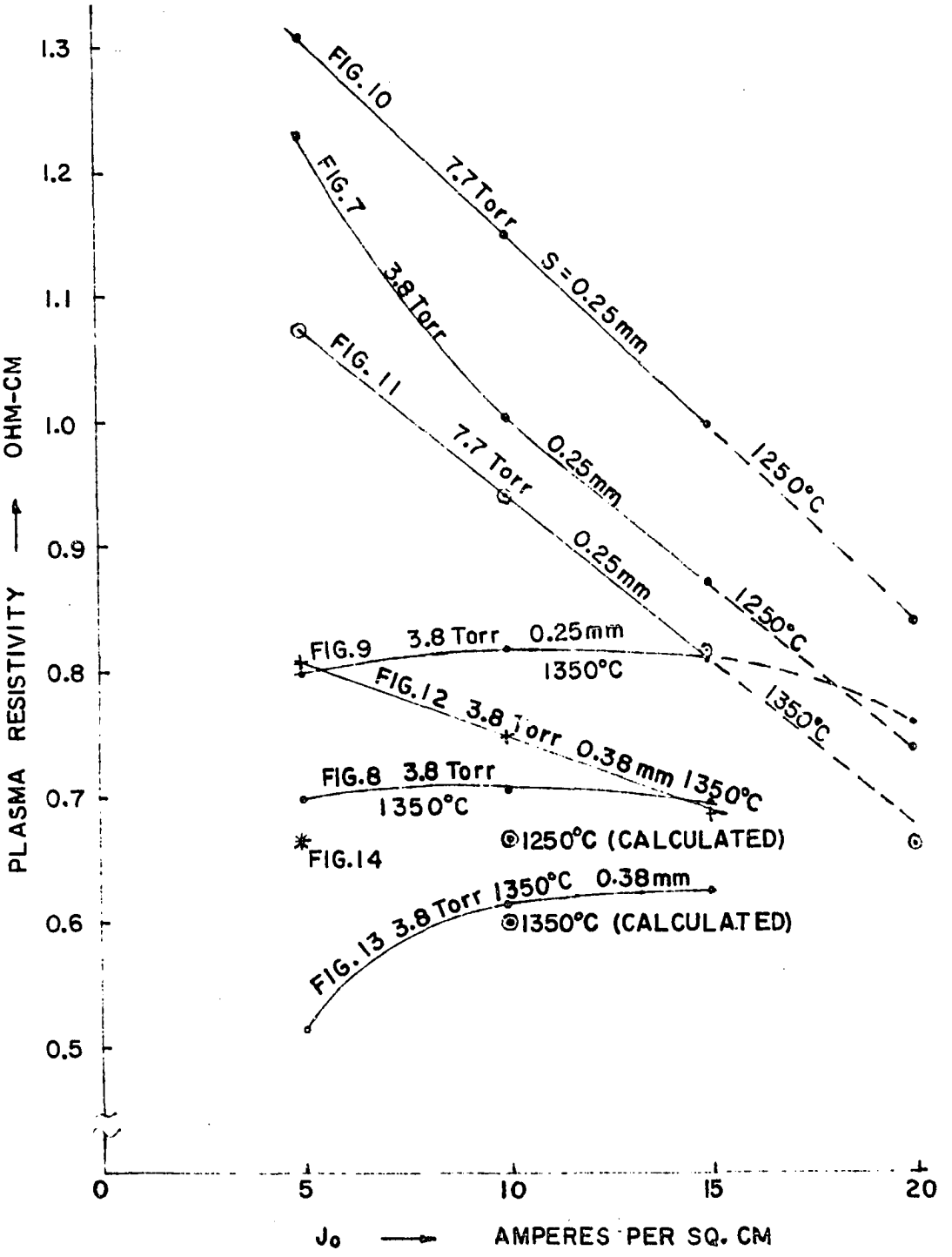

FIGURE 6. MEASURED PLASMA RESISTIVITY

In applying these yet well established theorems to engineering problems one would trace back to every initial assumptions. The Spitzer-Harm (2b) treatment of plasma resistivity employs statistical methods for a ionized gas at equilibrium state with no temperature gradient. This method seems still applicable to thermionic energy converters during the transient process for that the plasma is at low temperature, low energy and less turbulent than that of other kinds of applications. Furthermore, the cesium plasma behaves quite close to a Lorentz gas (6) in that the weight of cesium ions is 2.418×10^5 times than that of the electrons. This also implies the assumption that the distribution function of cesium ions is essentially unperturbed during the process.

In the process of deriving the plasma resistance, inductance and capacitance we decoupled some related effects. Symmetrical and hypothetical boundary conditions are used in the capacitance calculation in order to get a usable solution. These are certainly not fully justified, however, have been general feasible technique. The evaluated parameters were checked fairly well against obtainable experimental data.

In computing the plasma resistivity from equation (31), the electron temperature was approximated by the emitter temperature. The latter in reality represents the electron temperature at the emitter sheath. However, the emitter sheath was eliminated immediately after the pulsed discharge, thus the mean electron temperature of the plasma may be represented by the emitter temperature. The ideal method would be to insert a Langmuir probe to determine the electron temperature, but the spacings of practical diodes are so short that the probe would highly distort the electric field. It might also lead to the perturbations of other parameters. The

calculated plasma resistivity as compared to that of the measured agree within a factor of 2 (See Figure 6). The deviations are attributed to the scattering of neutrals. In general the results are reasonable for the present state of the art.

The foregoing mentioned plasma resistivity are basically at the equilibrium state. To investigate its transient properties one would also try to evaluate the dynamic resistance of the diode from its V-I characteristics. Under certain operating conditions, such as the ignited mode shown in Figures 8 and 12 of the Appendix, the dynamic resistance of the diode seemed to be zero. Furthermore, these regions are characterized by having ion-rich plasma in the interelectrode space. As a result, the diode tends to support low frequency instabilities caused by ion oscillations (15).

The resistance, inductance and capacitance of the plasma as evaluated are lumped parameters and analogous to a simple electric circuit. It appears that the R-L-C parallel circuit may best describe the plasma model since these parameters were derived independently. The other possibility is the R-L series branch in parallel with the capacitance. The frequencies of oscillation obtained in both cases are the same since the plasma resistance is rather low. The oscillation of the electron current in the resonant circuit simulates the electron oscillation in the plasma at high frequencies.

A numerical illustration is in order. First, we note that the plasma frequency or so called Langmuir frequency is given by equation (48). For an electron density n_e of 4×10^{12} per cm^3, the plasma frequency f_p is

1.8×10^{10} cycles per second. Referring to section II-B, the plasma R, L and C values are 5.45×10^{-3} ohm, 5.45×10^{-7} henry and 10.7×10^{-12} farad, respectively, for which the resonant frequency f_r of the circuit is 6.6×10^{7} cycles per second. The deviation is mainly due to the approximations made in computing the plasma capacitance. The sheath thickness ω/ν_o at high frequencies is comparable to the electrode spacing L, thus the effective permittivity ϵ_{eff} in equation (69) will be reduced. This in turn yields a smaller capacitor. In addition, the solution is valid only when $\omega < 3/4$, i.e. when the applied frequency is less than 3/4 of the plasma frequency. For ω approaching 1, it may be shown (14) that the effective permittivity is approximated by

$$\epsilon_{eff} = 1 - \frac{1}{\omega^2}$$

In effect, the plasma capacitance is highly sensitive to the frequency when $\omega \rightarrow 1$, and becomes a blockade capacitor as $\omega = 1$ ($Z_c \rightarrow \infty$). This interpretation suggests that the resonant frequency ω_r should be slightly lower than the plasma frequency ω_p, which agrees to the model of dissipative parallel circuits.

The plasma reactance was determined from the decay constant reported in two experiments (10, 11). The order of magnitude seemed to be correct and no other quantitative prediction of this parameter has been reported.

The area for possible future research would be to reconsider some effects neglected in this dissertation. The transition between the extinguished mode and the ignited mode may be investigated. This is certainly a physics problem but the plasma inductance and capacitance might play a role in this resonant phenomenon. As to the experimental work,

there is a great deal that might be done. The information and experience in this area is urgently needed for the future large-scale direct-energy conversion.

IV. SELECTED REFERENCES

1. Kaplan, C. Investigation of the current density limitations in a thermionic energy converter. Marquardt Corporation Report No. 25, 114. 1963.

2a. Hapsopoulos, G. Transport effects in cesium thermionic converters. Institute of Electrical and Electronic Engineers Proceedings 51: 725-733. 1963.

2b. Spitzer, L., Jr. Physics of fully ionized gases. Interscience Publishers, Inc. New York. 1962.

3. Pariser, B. and R. A. Gross. A cesium plasma diode. Plasma Laboratory, Columbia University. New York. 1963.

4. Talaat, M. E. Generalized theory of the thermionic energy converter. American Institute of Electrical Engineers Transactions Application and Industry 63: 309-319. 1962.

5. Suits, C. G. and H. E. Way, Editors. The collected works of Irving Langmuir. Volume 5. Plasma and oscillations. Pergamon Press. New York. 1961.

6. Cohen, R. C., L. Spitzer, Jr. and P. McR. Routly. The electrical conductivity of an ionized gas. Physical Review 80: 230-238. 1950.

7. Chapman, S. C. and T. G. Cowling. The mathematical theory of non-uniform gases. Cambridge University Press. Cambridge, England. 1939.

8. Robinson, L. B. Thermodynamic and transport properties of a cesium plasma. Advanced Energy Conversion 3, No. 1: 19-36. 1963.

9. Fouad, A. A. Notes on thermionic energy conversion. Unpublished Dittoed notes for Electrical Engineering Special Topics Course, Winter 1962. Department of Electrical Engineering, Iowa State University of Science and Technology. Ames, Iowa. 1963.

10. Firle, T. E. Observations of current decay in an isothermal cesium cell. Conference on Physical Electronics Report 21: 141-145. 1961.

11. Laubenstein, R. A., C. Kaplan, S. Schneider and J. Creedon. Sources of positive ions for space charge neutralization at low temperatures. Advanced Energy Conversion 3: 351-361. 1963.

12. Sheldon, J. W. Mobilities of the alkali metal ions in their own vapor. Journal of Applied Physics 34: 444. 1963.

13. Brown, R. G., R. A. Sharpe and W. L. Hughes. Lines, waves and antennas. Ronald Press Co. New York. 1961.

14. Shure, F. C. Boundary value problems in plasma oscillations; the plasma capacitor. Plasma Physics (Journal of Nuclear Energy, Part C) 6: 1-14. 1964.

15. Zollweg, R. J. and M. Gottlieb. Radio-frequency oscillations in thermionic diodes. Institute of Electrical and Electronics Engineers Proceedings 51: 754-759. 1963.

16. Rocard, J. M. and G. W. Paxton. Relaxation oscillations in a plasma diode. Journal of Applied Physics 32: 1171-1172. 1961.

V. ACKNOWLEDGEMENTS

The author wishes to thank his major professor, Dr. J. E. Lagerstrom, for his invaluable help and encouragement throughout the work on this thesis. He is also indebted to Dr. A. A. Fouad and many other members of the Department of Electrical Engineering for their advice and assistance. Also his many thanks and appreciation to Dr. N. S. Rasor of Thermo Electron Engineering Corporation, who suggested this topic, and to Mr. C. Kaplan of Marquardt Corporation, for his kindness and permission to use his experimental data.

VI. APPENDIX

The steady-state and transient curves from Reference 1 are shown in Figures 7 to 14.

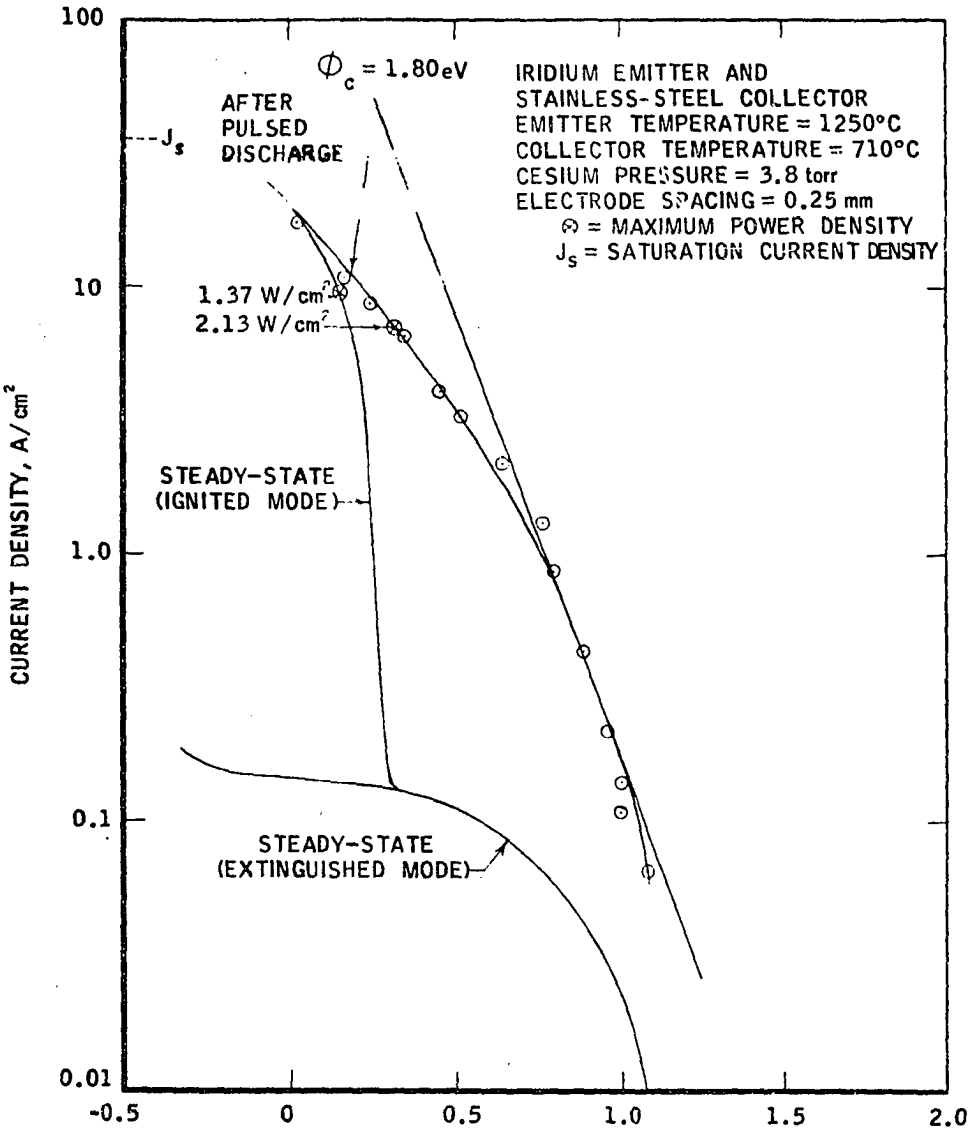

FIGURE 7. EXPERIMENTAL V-I CURVES

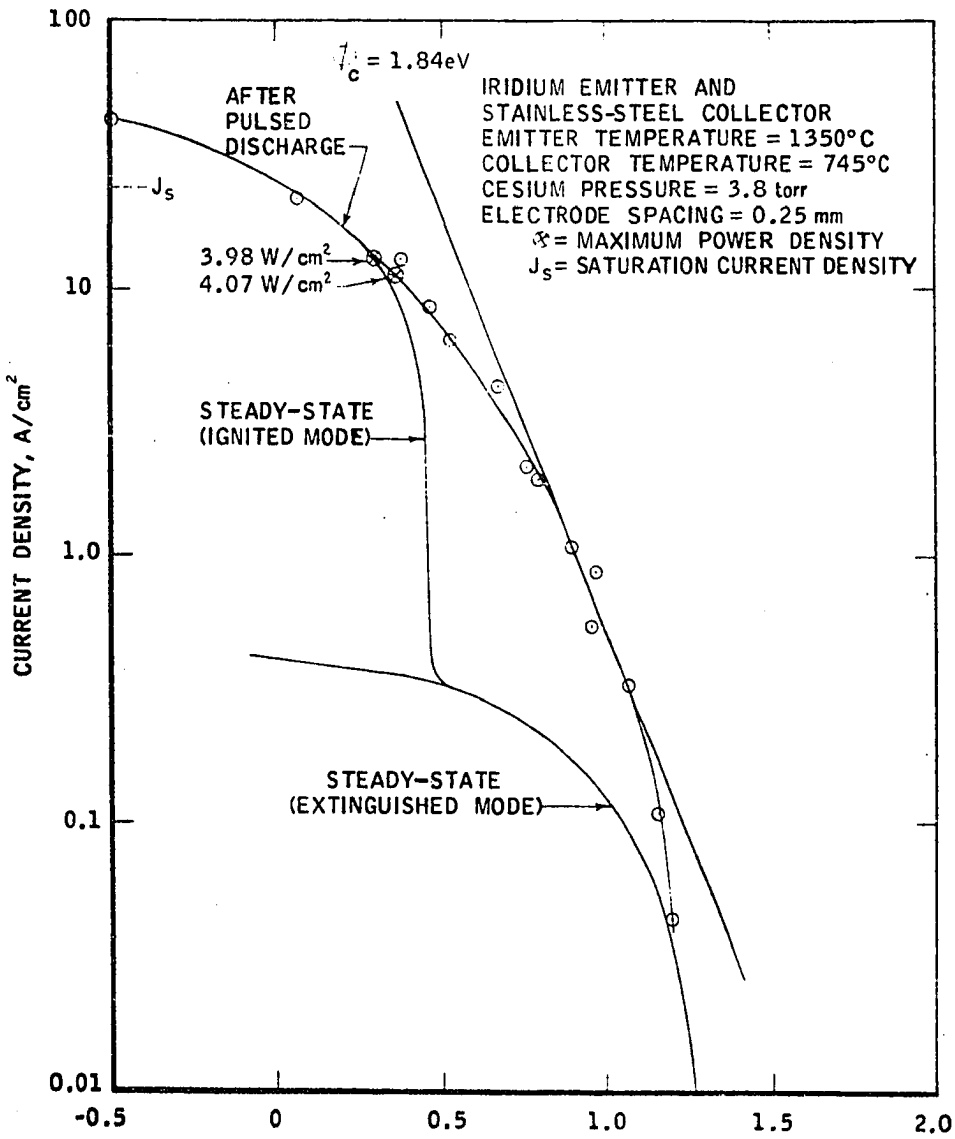

FIGURE 8. EXPERIMENTAL V-I CURVES

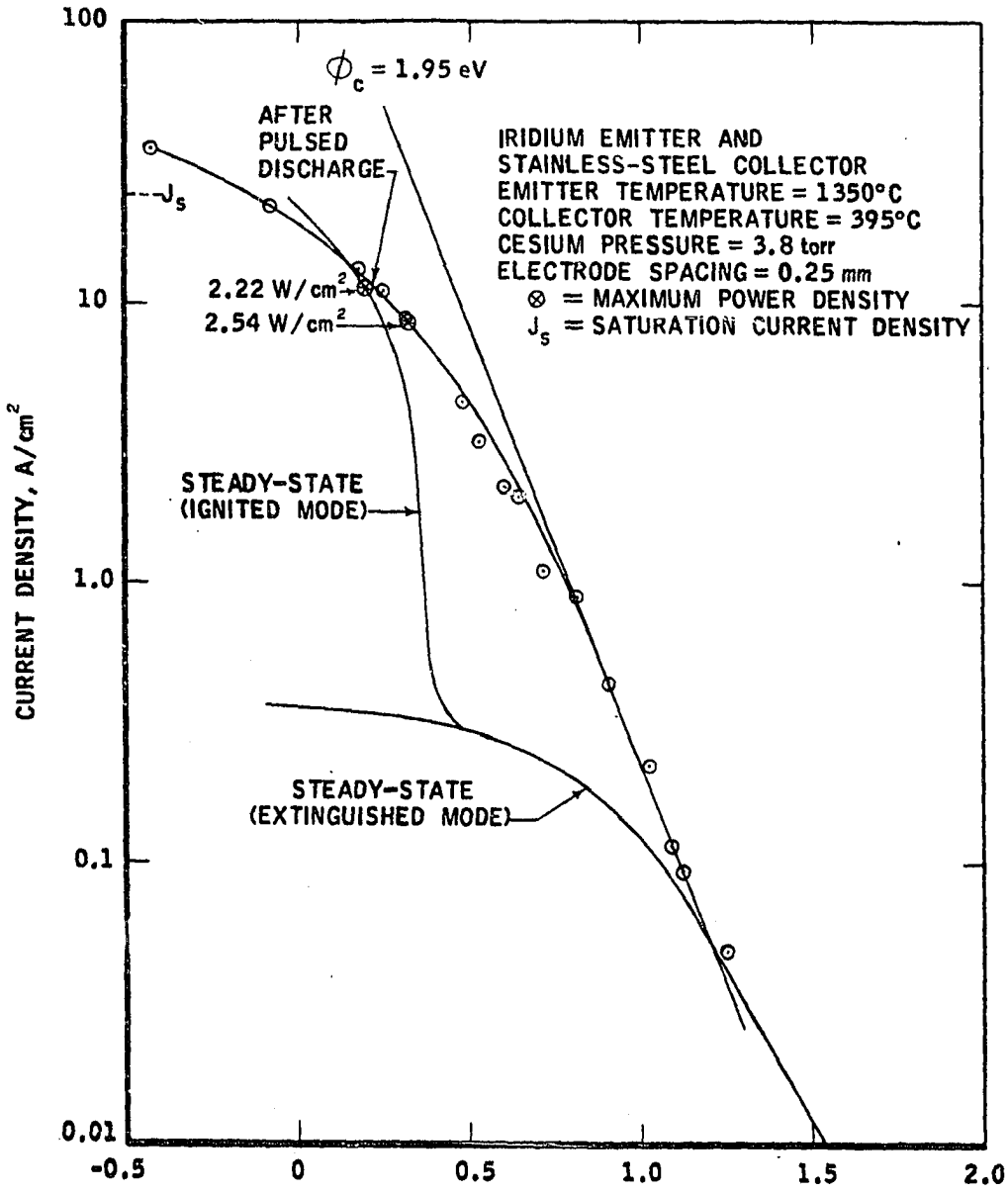

FIGURE 9. EXPERIMENTAL V-I CURVES

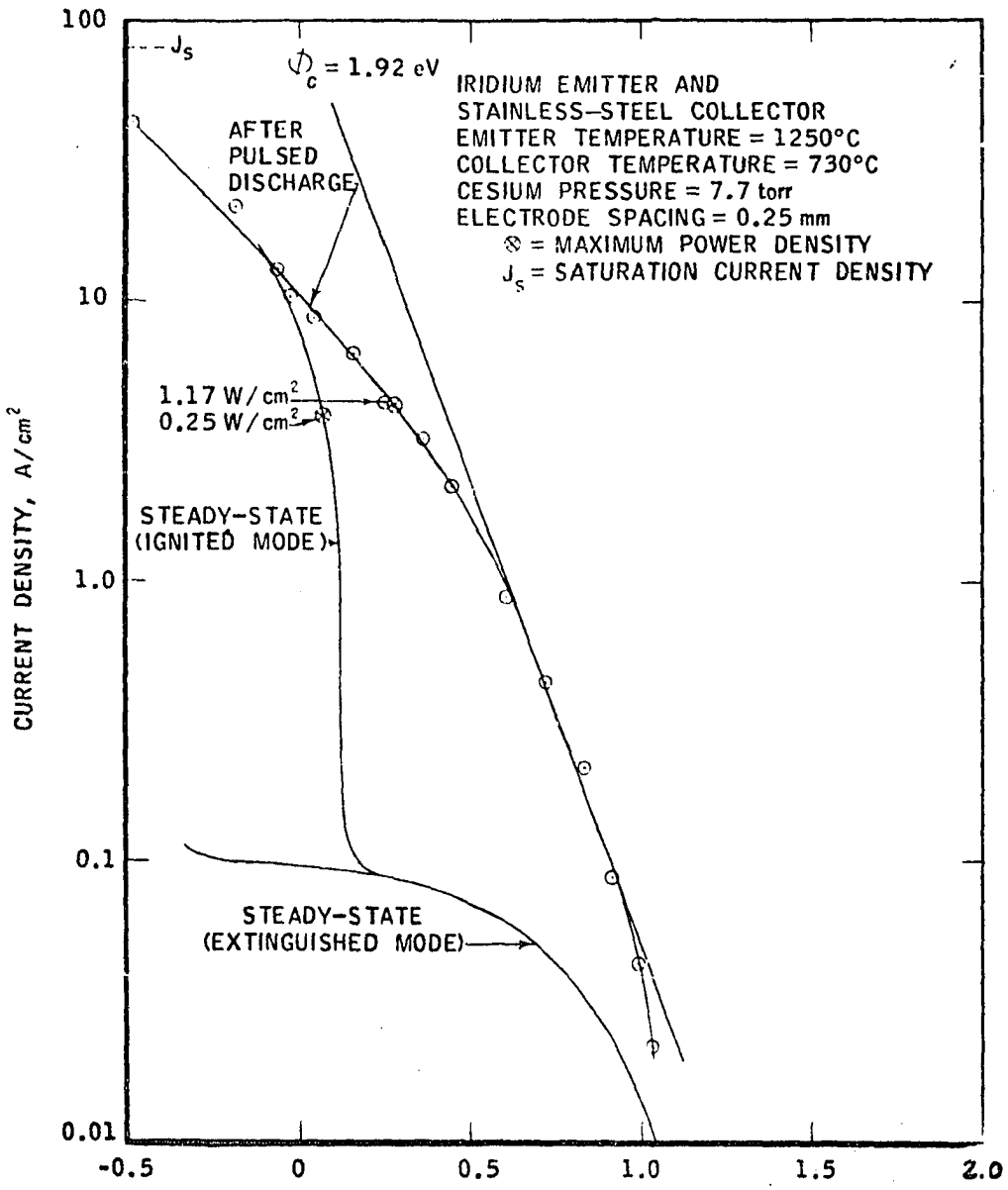

FIGURE 10. EXPERIMENTAL V-I CURVES

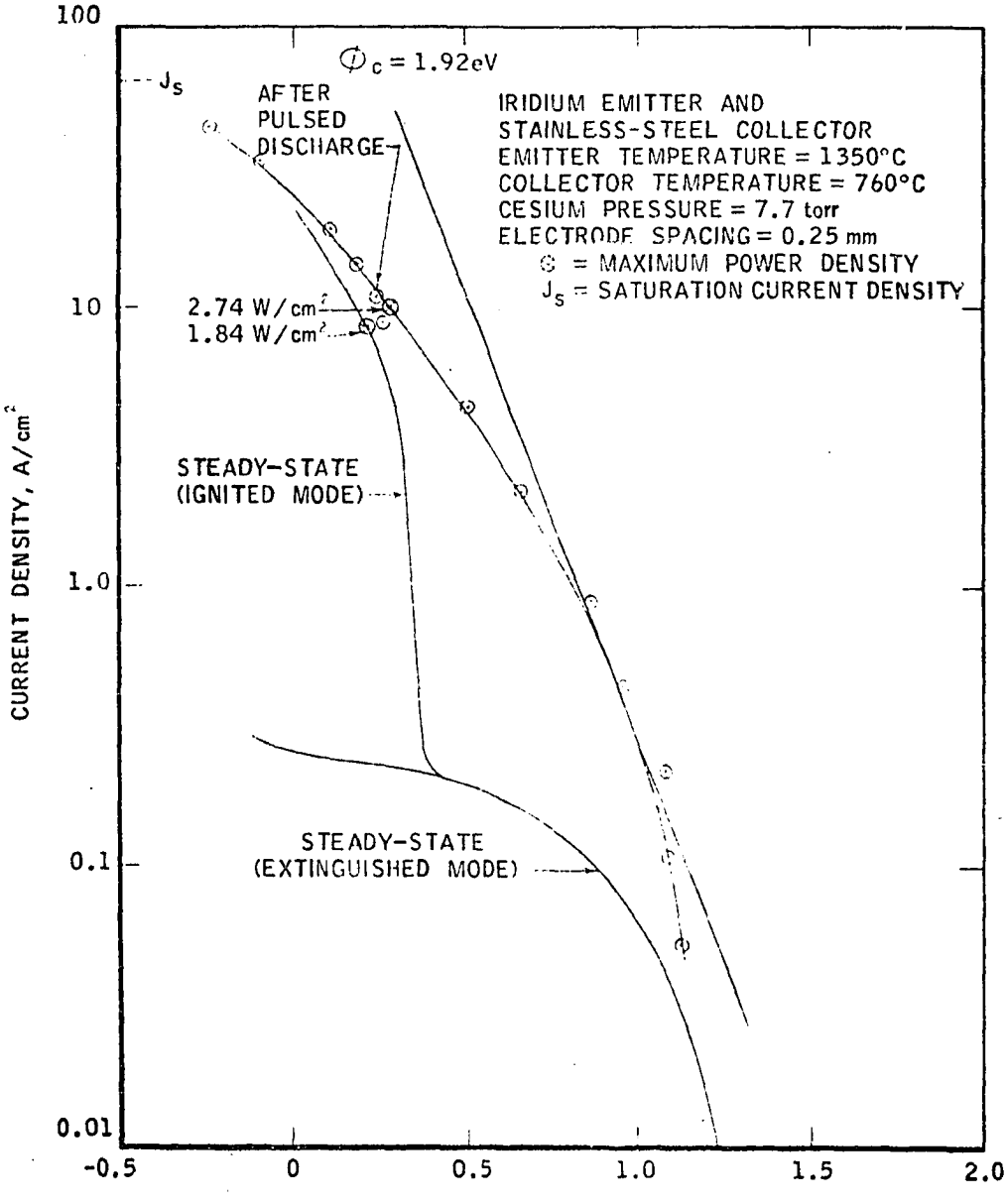

FIGURE II. EXPERIMENTAL V-I CURVES

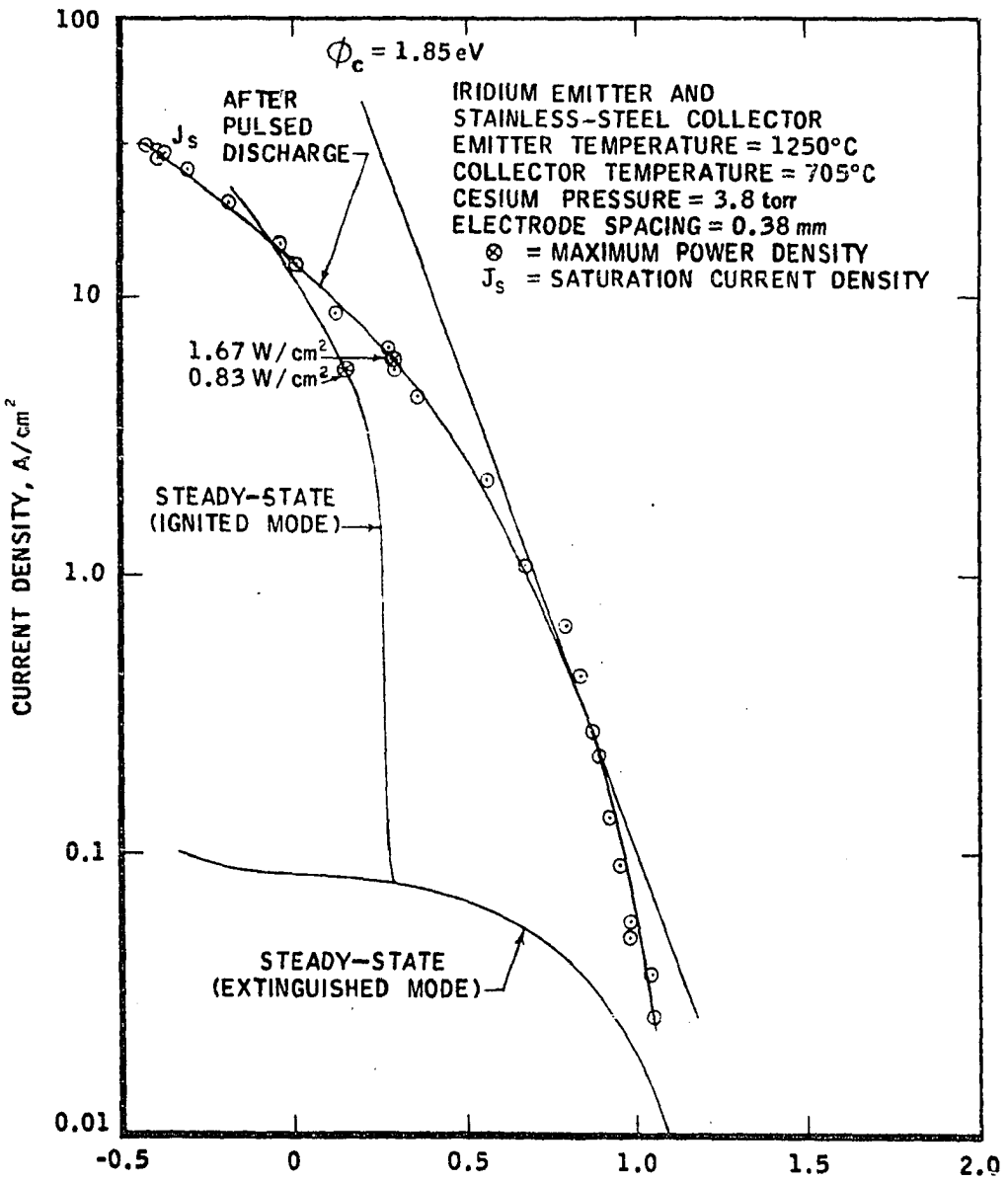

FIGURE 12. EXPERIMENTAL V-I CURVES

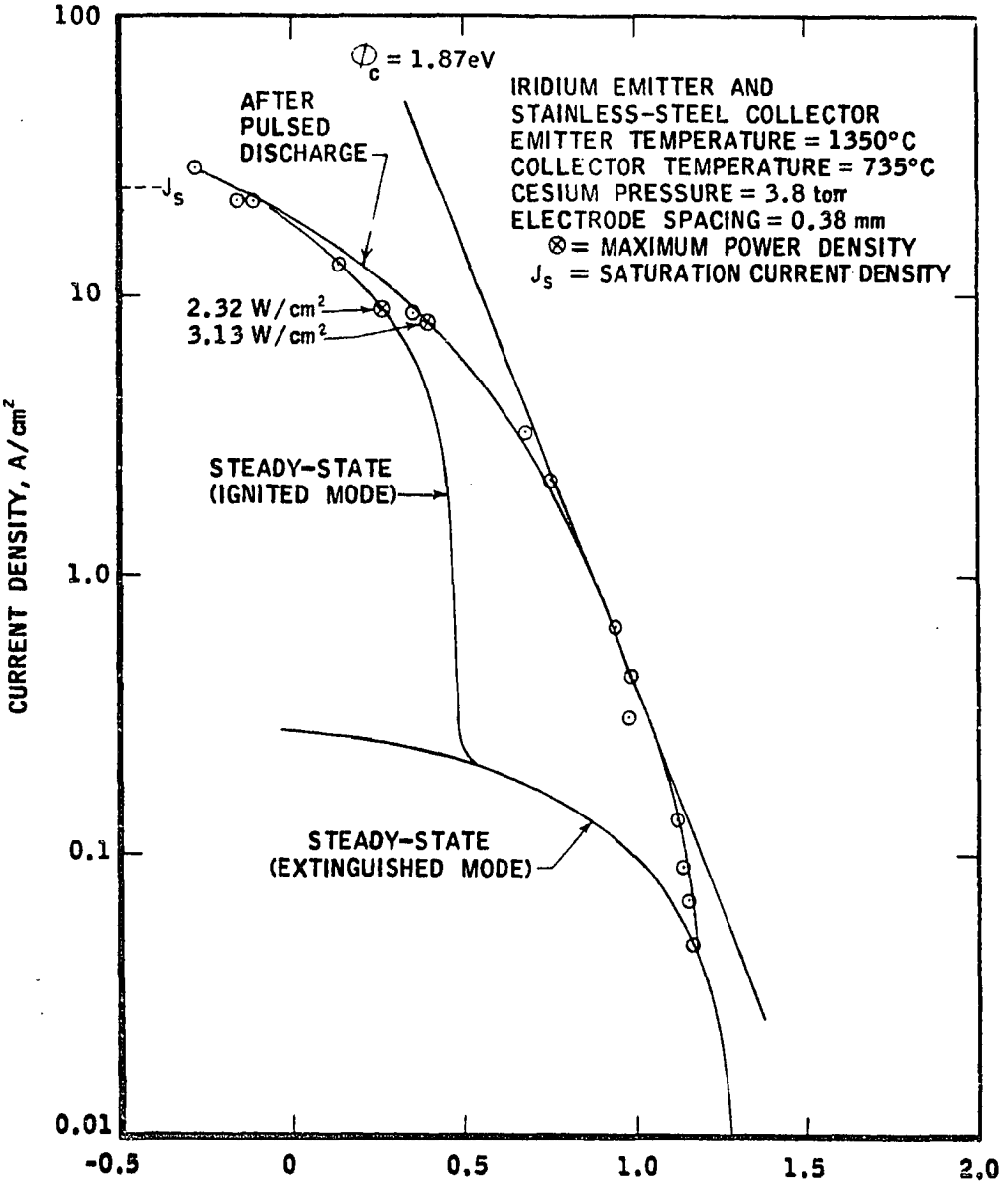

FIGURE 13. EXPERIMENTAL V-I CURVES

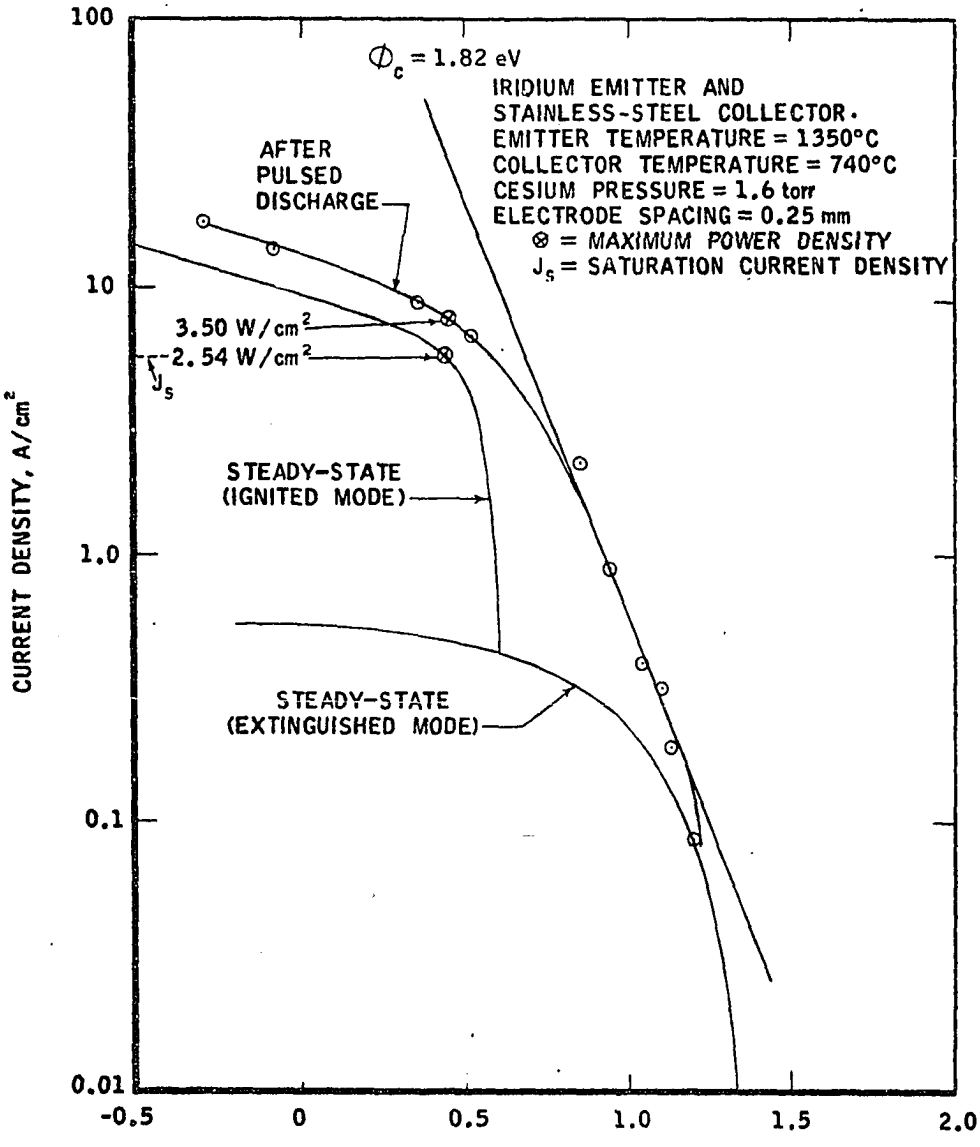

FIGURE 14. EXPERIMENTAL V-I CURVES